

Modelling and simulation of a trickling filter bioreactor for ex-situ hydrogenotrophic methanation^{*}

Ortiz-Ricárdez, F.A., Muñoz-Páez, K.M., Vargas, A.*

** Laboratory for Research on Advanced Processes for Water Treatment, Unidad Académica Juriquilla, Instituto de Ingeniería, UNAM. (e-mail: AVargasC@iingen.unam.mx).*

Abstract:

A mathematical modelling approach for a hydrogenotrophic methanation process in a trickling filter bioreactor (TFB) is formulated and simulated. As other works have suggested, the proposed model partitions the physical space in an arbitrary number of vertical levels and uses the first Fickian diffusion law along its vertical axis and along the thickness of the biofilm layer attached to the inert bed material. The biological hydrogenotrophy reaction is modelled using Monod kinetics. According to the ideal gas law, to calculate gas flows among levels, the model approach considers the fixed amount of moles of gas in each TFB level. Simulations of the proposed model were compared to experimental results of ex-situ hydrogenotrophic methanation in a TFB. Model performance against the experimental results of the real reactor fitted remarkably well the effluent proportions within an average 2% error band in the reported best experimental case. It even surpassed real productivity by 20% on average, considering an ideal scenario in which the model formulation assumes that hydrogenotrophic methanation by archaea is the sole biological transformation. A qualitative analysis of important model parameters was crucial for fitting simulation results to real experimental data. Particularly, influent raw biogas proportions near the ideal stoichiometry for hydrogenotrophic methanation is detrimental to purity and productivity of the desired biomethane effluent. The numerical effort needed for simulations was remarkably lower than expected, given the large-sized models the approach may produce. Simulation results provided insight into possible model modifications for further discussion.

Keywords: Modeling and identification, Parameter and state estimation, Monitoring, Dynamics and control, Bioenergy production.

1. INTRODUCTION

Trickling filter bioreactors (TFB) are often used as pollutant removal schemes in water and gas treatment. Computer fluid dynamics (CFD) has been used to study the mass transfer processes occurring in biotrickling filters; the resulting distributed parameter models that are founded on partial differential equations derived from the Navier-Stokes' equations may describe precisely the fluid dynamics involved (Markthaler et al., 2020). However, for control purposes, simpler models are more appealing to help establish control directives on variables that can directly be handled via an online actuator, such as a modification of the gaseous and/or hydraulic retention times; hence, lumped-parameter models made of ordinary algebraic-differential equations are preferred.

Hydrogenotrophic methanation is a process for refining biogas in which archaea metabolize hydrogen (H_2) and carbon dioxide (CO_2) to produce methane (CH_4) as a metabolite (Burkhardt and Busch, 2013). Raw biogas contains mostly CO_2 and CH_4 as predominant compo-

nents, present in volumetric concentrations of CH_4 between 53–70%, and between 30–47% of CO_2 originated from anaerobic digestion of sewage sludge, livestock manure or agroindustrial biowastes (Muñoz et al., 2015). Afterwards, raw biogas is converted into biomethane, whose composition complies with the natural gas quality on the market, and is straightforwardly transported in available infrastructure for natural gas. Volumetric proportions of minimum 95% (Swinbourn et al., 2024), and even 90% of CH_4 as per up-gradation standard IS 16087:2016 (Katariya and Patolia, 2023), is the criterion for denominating the processed biogas as biomethane.

A successful method for enhancing biomethane from raw biogas was experimentally tested by Muñoz-Páez et al. (2025), favouring biomethane productivity using raw biogas $H_2:CO_2$ with low volumetric ratios of around 4:3; hence the formulation of a mathematical model is appealing for systematically studying such an advantageous process and proposing feedback control laws for increasing productivity and/or purity, as well as for robustification. Modelling approaches based on the first Fickian diffusion law and the segmentation into levels of the trickling bed, as proposed by Dupnock and Deshusses (2021), serve as starting point of this work, but in addition, the physical restriction of

* Work supported by UNAM Postdoctoral Program (POSDOC); project IIUNAM-GII-3406; CONAHCYT frontier science grant CF-2023-I-537; and Mexican Researchers Program (ID 6407, project 265)

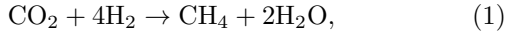
a maximum total number of moles in a given TFB level volume according to the ideal gas law is considered.

The objective of this paper is to mathematically model a hydrogenotrophic methanation process in a trickling filter-based reactor, and to numerically simulate such model to compare its performance against the experimental results of the real reactor set up by Muñoz-Páez et al. (2025). The proposed model considers gaseous diffusion transport through the trickling filter, the mass transfer among liquid and gaseous phases, and also the reaction of absorbed gases in the biofilm attached to the bed. Wet (i.e. completely soaked) and moist (i.e. sufficiently humidified) biofilms, gas volume conversion from H_2 and CO_2 into CH_4 , and axial dispersion are all included in the model.

This paper is organized as follows: Section 2 presents the TFB scheme and its proposed model structure divided in 4 submodels: gaseous, liquid, biofilm, and the important aspect of combined diffusion and mass transfer. Section 3 shows the model simulation and its numerical performance; some key aspects for its coarse and fine tuning are discussed for fitting experimental results of ex-situ biomethanation carried out by Muñoz-Páez et al. (2025). Finally, conclusions and possible model improvements are outlined in Section 4.

2. MODEL STRUCTURE

The TFB is assumed to be fed with a gas flow from below and with a liquid flow from above that recirculates from the bottom, and the gaseous outflow is assumed to exit the system from above (see Fig. 1). The TFB was filled with high density polyethylene rings in a packed volume of 0.7 L (Muñoz-Páez et al., 2025). In addition, the hydrogenotrophic methanation reaction is stoichiometrically described by (Gujer and Zehnder, 1983)



where resulting gaseous and liquid volumetric proportions of H_2O are meaningless compared to the total recirculated liquid volume; thus, they are conventionally disregarded.

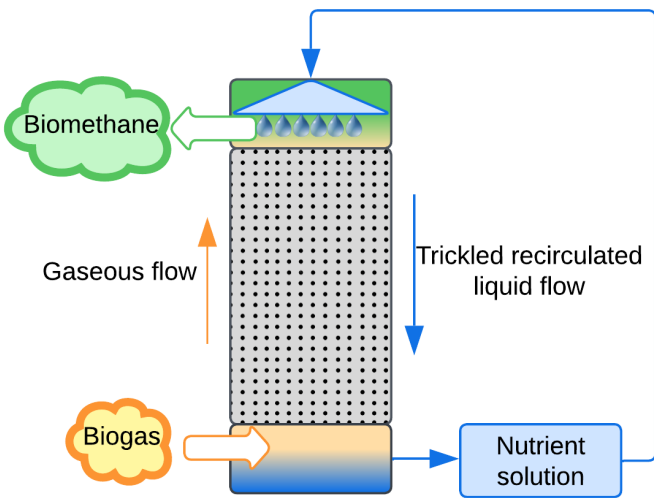


Fig. 1. TFB scheme.

The proposed model considers the following important assumptions:

- The TFB is modeled with n vertical levels, indicated with the subscript i , such that $i = 1$ is the lowermost level and $i = n$ the uppermost one; the total volume of each level (contained in the center dashed square of Fig. 2) is fixed.
- On each level i , 4 media coexist divided in layers: a gas phase (one layer), a liquid phase (one layer), and two types of biofilm with p layers, where the active biomass is only present. These are: wet biofilm, in contact with the layer of liquid phase, and moist biofilm, in contact with the gas phase (actually the liquid layer is assumed irrelevantly thin). Index used for all layers is j , so $j = 1$ is the innermost layer of moist biofilm, $j = p + 1$ is the gas phase, $j = p + 2$ is the liquid phase and $j = 2p + 2$ is the innermost layer of wet biofilm.
- Components are the gases or other metabolites (if needed); currently only 3 are represented by index $k \in \{1, 2, 3\}$ for CH_4 , CO_2 and H_2 , respectively.
- Concentrations for k -th component, at the i -th level, in the j -th layer or phase are represented by $C_{j,k,i}$; this quantity may have units g/L , kg/m^3 , etc.
- The volume a gas can occupy in a level is $V_{G,i}$ and assumed constant; hence, volumes for liquid, inert material bed and biofilm in a level are also constant.
- Biomass transfer between levels and layers, and biological reaction in the liquid phase are non-existent.

For ease of presentation in this paper, indices $j = p + 1$ and $j = p + 2$ are sometimes replaced by G and L to emphasize that it is the gas or the liquid phase, while indices $j = p$ and $j = p + 3$ are replaced by M and W for the outermost layer of the moist or wet biofilm, respectively.

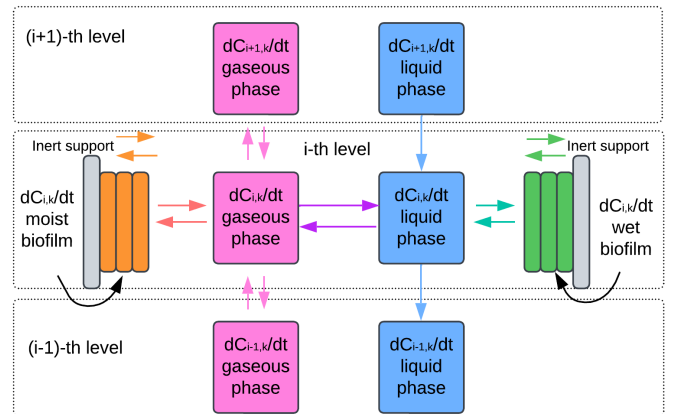


Fig. 2. TFB levels and interactions between layers.

Involved gases follow the ideal gas law $PV = nRT$, where P is the absolute pressure in bar, T is the absolute temperature in K, V is the volume occupied by that gas in L, $R = 0.08314462$ is the ideal gas constant in $L \cdot \text{bar} / K / \text{mol}$. The ideal gas law is also valid for a gaseous mix in which $n = \sum_k n_k$, where n_k is the amount in moles of each individual gas. Thus, for the k -th gas, then $n_k M_k$ is the *mass in grams*, where M_k is the average molar mass of the gas in g / mol . Hence, *molar concentration* of the k -th gas in a given volume is $C_{G,k,i} / M_k = n_k / V_{G,i}$, where n_k is the number of moles of the k -th gas in the gaseous volume $V_{G,i}$ of the i -th level. In addition, the total number of moles

of a gas mixture in a fixed volume at a certain pressure and temperature is *constant* at any level and given by

$$\sum_{k=1}^m \frac{C_{G,k,i}}{M_k} = \frac{P_{atm}}{RT_0}. \quad (2)$$

2.1 Gaseous model

Let the process be isobaric at P_{atm} and isothermic at T_0 . Let $V_{G,i}\Gamma_{k,i}(t)$ be the rate of change in mass due to *combined diffusion and mass transfer* phenomena (see below) for the k -th gas in the i -th level, where

- $V_{G,i}$ is the volume of gas in the i -th level of the TFB, assumed to be constant and known;
- $\Gamma_{k,i}(t)$ is the rate of change of the concentration of the k -th gas in the i -th level due to *combined diffusion and mass transfer* processes; its units are g/L/h.

Therefore the number of moles of the k -th gas increasing or decreasing after time Δt due to rate $\Gamma_{k,i}(t)$ is¹

$$\Delta n_{k,i,d} = V_{G,i} \left(\frac{\Gamma_{k,i}}{M_k} \right) \Delta t. \quad (3)$$

Conversely, let us assume a positive inflow of gas with rate $Q_{G,i-1}$ from the $(i-1)$ -th level below and a positive outflow with rate $Q_{G,i}$ to the $(i+1)$ -th level above. Notice that these flows imply that the volume increasing or decreasing after time Δt are $Q_{G,i-1}\Delta t$ or $Q_{G,i}\Delta t$, respectively; hence, the amount of mass entering or leaving the level depends on where it comes from, summarized in the following 4 cases:

- (1) $Q_{G,i-1} > 0$ and $Q_{G,i} > 0$ (usual and desired): moles of k -th gas added to the volume $V_{G,i}$ come from the $(i-1)$ -th level, and moles are subtracted from the level itself²:

$$\Delta n_{k,i,f} = \left(\frac{C_{G,k,i-1}}{M_k} \right) |Q_{G,i-1}| \Delta t - \left(\frac{C_{G,k,i}}{M_k} \right) |Q_{G,i}| \Delta t. \quad (4)$$

- (2) $Q_{G,i-1} > 0$ and $Q_{G,i} < 0$ (net consumption of mass in the level): both entries are positive, because moles are added both from the levels above and below:

$$\Delta n_{k,i,f} = \left(\frac{C_{G,k,i-1}}{M_k} \right) |Q_{G,i-1}| \Delta t + \left(\frac{C_{G,k,i+1}}{M_k} \right) |Q_{G,i}| \Delta t. \quad (5)$$

- (3) $Q_{G,i-1} < 0$ and $Q_{G,i} < 0$ (gas flow is reversed): moles are added from the level above and subtracted from the level itself:

$$\Delta n_{k,i,f} = - \left(\frac{C_{G,k,i}}{M_k} \right) |Q_{G,i-1}| \Delta t + \left(\frac{C_{G,k,i+1}}{M_k} \right) |Q_{G,i}| \Delta t. \quad (6)$$

- (4) $Q_{G,i-1} < 0$ and $Q_{G,i} > 0$ (net production despite withdrawal): moles are subtracted from the level to go to the levels below and above:

$$\Delta n_{k,i,f} = - \left(\frac{C_{G,k,i}}{M_k} \right) |Q_{G,i-1}| \Delta t - \left(\frac{C_{G,k,i}}{M_k} \right) |Q_{G,i}| \Delta t. \quad (7)$$

Differential equations for each gas concentration can be derived by considering that change in concentration of the k -th gas is given by

$$\Delta C_{G,k,i} = \frac{M_k}{V_{G,i}} (\Delta n_{k,i,d} + \Delta n_{k,i,f}) \quad (8)$$

and henceforth

$$\dot{C}_{G,k,i} = \lim_{\Delta t \rightarrow 0} \Delta C_{G,k,i} / \Delta t \quad (9)$$

becomes either of the following:

$$\dot{C}_{G,k,i} = \Gamma_{k,i} + \frac{1}{V_{G,i}} (C_{G,k,i-1} |Q_{G,i-1}| - C_{G,k,i} |Q_{G,i}|), \quad (10)$$

if $Q_{G,i-1} > 0$ and $Q_{G,i} > 0$;

$$\dot{C}_{G,k,i} = \Gamma_{k,i} + \frac{1}{V_{G,i}} (C_{G,k,i-1} |Q_{G,i-1}| + C_{G,k,i+1} |Q_{G,i}|), \quad (11)$$

if $Q_{G,i-1} > 0$ and $Q_{G,i} < 0$;

$$\dot{C}_{G,k,i} = \Gamma_{k,i} + \frac{1}{V_{G,i}} (-C_{G,k,i} |Q_{G,i-1}| + C_{G,k,i+1} |Q_{G,i}|), \quad (12)$$

if $Q_{G,i-1} < 0$ and $Q_{G,i} < 0$;

$$\dot{C}_{G,k,i} = \Gamma_{k,i} + \frac{1}{V_{G,i}} (-C_{G,k,i} |Q_{G,i-1}| - C_{G,k,i} |Q_{G,i}|), \quad (13)$$

if $Q_{G,i-1} < 0$ and $Q_{G,i} > 0$.

To decide the value of $Q_{G,i}$ given the value of $Q_{G,i-1}$, it must be considered that at every instant the total change in the number of moles in the fixed gaseous space volume always add up to zero, i.e.

$$\sum_{k=1}^m (\Delta n_{k,i,d} + \Delta n_{k,i,f}) = 0. \quad (14)$$

In addition, it must be noticed that all previously analyzed 4 cases of $\Delta n_{k,i,f}$ can be summarized as

$$\Delta n_{k,i,f} = \left(\frac{C_{G,k,a}}{M_k} \right) Q_{G,i-1} \Delta t - \left(\frac{C_{G,k,b}}{M_k} \right) Q_{G,i} \Delta t \quad (15)$$

where we respect the sign convention for the flows $Q_{G,i-1}$ and $Q_{G,i}$ and (a, b) is $(i-1, i)$, $(i-1, i+1)$, $(i, i+1)$, or $(i, i+1)$ for the first, second, third or fourth case, respectively; hence

$$\begin{aligned} \sum_{k=1}^m \Delta n_{k,i,f} &= \left[Q_{G,i-1} \sum_{k=1}^m \frac{C_{G,k,a}}{M_k} - Q_{G,i} \sum_{k=1}^m \frac{C_{G,k,b}}{M_k} \right] \Delta t \\ &= \left(\frac{P_{atm}}{RT_0} \right) (Q_{G,i-1} - Q_{G,i}) \Delta t, \end{aligned} \quad (16)$$

where we have used the equality (2). Then the *gas flow rate* from the i -th level is computed by substituting (3) and (16) in (14):

$$\left(\frac{P_{atm}}{RT_0} \right) (Q_{G,i} - Q_{G,i-1}) = V_{G,i} \sum_{k=1}^m \frac{\Gamma_{k,i}}{M_k}. \quad (17)$$

This leads to

$$Q_{G,i} = Q_{G,i-1} + V_{G,i} S_i, \quad (18)$$

with quantity S_i defined as

$$S_i \triangleq \left(\frac{RT_0}{P_{atm}} \right) \sum_{k=1}^m \frac{\Gamma_{k,i}}{M_k}. \quad (19)$$

¹ The d subindex is for *diffused*.

² The f subindex is for *fed* and absolute values are used for flow rates to emphasize addition or subtraction.

Eq. (18) allows to compute the gas flow from/to the i -th level for any sign of the gas flow to/from the previous level. Under this convention, we can first compute the sign of each $Q_{G,i}$ and assign a boolean index $d_i = 0$ if $Q_{G,i} \geq 0$, or $d_i = 1$ if $Q_{G,i} < 0$ (the ‘‘anomalous’’ case), and then use it to define which concentration value to use in the differential equations in the gas phase, which become

$$\dot{C}_{G,k,i} = \Gamma_{k,i} + C_{G,k,(i-1+d_{i-1})} \frac{Q_{G,i-1}}{V_{G,i}} - C_{G,k,(i+d_i)} \frac{Q_{G,i}}{V_{G,i}}, \quad (20)$$

wherein substituting (18), they become

$$\dot{C}_{G,k,i} = \Gamma_{k,i} + (C_{G,k,(i-1+d_{i-1})} - C_{G,k,(i+d_i)}) \frac{Q_{G,i-1}}{V_{G,i}} - C_{G,k,(i+d_i)} S_i, \quad (21)$$

which are expressions in terms of only the previous level gas flow $Q_{G,i-1}$; this is summarized in Table 1. In this generalization, we take $C_{G,k,0}$ as the concentrations in the influent gas and $C_{G,k,n+1}$ as the concentrations in the space where the gas vents with the outflow.

Table 1. Gas concentrations to use depending on gas flows.

$Q_{G,i-1}, Q_{G,i}$	(d_{i-1}, d_i)	$C_{G,k,(i-1+d_{i-1})}$	$C_{G,k,(i+d_i)}$
$(\geq 0, \geq 0)$	$(0, 0)$	$C_{G,k,i-1}$	$C_{G,k,i}$
$(\geq 0, < 0)$	$(0, 1)$	$C_{G,k,i-1}$	$C_{G,k,i+1}$
$(< 0, < 0)$	$(1, 1)$	$C_{G,k,i}$	$C_{G,k,i+1}$
$(< 0, \geq 0)$	$(1, 0)$	$C_{G,k,i}$	$C_{G,k,i}$

2.2 Diffusion and mass transfer

The rates of change of concentration of each gas $\Gamma_{k,i}(t)$ due to combined diffusion and mass transfer must be computed to find the outflow rate and use it in the differential equation. Two phenomena are considered to model this rate:

- (1) The mass transfers of gas from this gas phase to the interphase with the liquid phase and to the interphase with the moist biofilm;
- (2) The axial diffusion between levels according to Fick’s first law.

Due to lack of space, equations for $\Gamma_{k,i}(t)$ for $i = 2, \dots, (n-1)$ are directly presented

$$\Gamma_{k,i}(t) = \frac{D_{\text{ax}}}{\delta^2} (C_{G,k,i-1}(t) - 2C_{G,k,i}(t) + C_{G,k,i+1}(t)) + k_G a \left(C_{L,k,i}(t) - \frac{2}{H_k} C_{G,k,i}(t) + C_{M,k,i}(t) \right), \quad (22)$$

and for $i = 1$ and $i = n$ the equations are

$$\Gamma_{k,1}(t) = -\frac{D_{\text{ax}}}{\delta^2} (C_{G,k,1}(t) - C_{G,k,2}(t)) + k_G a \left(C_{L,k,1}(t) - \frac{2}{H_k} C_{G,k,1}(t) + C_{M,k,1}(t) \right), \quad (23)$$

$$\Gamma_{k,n}(t) = \frac{D_{\text{ax}}}{\delta^2} (C_{G,k,n-1}(t) - C_{G,k,n}(t)) + k_G a \left(C_{L,k,n}(t) - \frac{2}{H_k} C_{G,k,n}(t) + C_{M,k,n}(t) \right), \quad (24)$$

where D_{ax} is the axial dispersion coefficient, δ is the height of each level in the TFB, $k_G a$ is the gas mass transfer coefficient, and H_k is Henry’s constant for the k -th gas.

2.3 Liquid model

For the liquid phase we consider that there is no bioreaction taking place in it and that $V_L = V_{L,i}$ for all $i = 1, \dots, n$. There is also no diffusion due to Fick’s first law. If the gas is supplied below the trickling filter (as we use in our laboratory), then the liquid and gas flows are in countercurrent and the levels are numbered from the bottom to the top i.e. $i = n$ is the uppermost level. Then for $i = 1, \dots, (n-1)$:

$$\dot{C}_{L,k,i} = k_G a \left(\frac{C_{G,k,i}}{H_k} - C_{L,k,i} \right) - k_L a (C_{L,k,i} - C_{W,k,i}) + \frac{Q_L(t)}{V_L} (C_{L,k,i+1} - C_{L,k,i}), \quad (25)$$

while for $i = n$, the equation is

$$\dot{C}_{L,k,n} = k_G a \left(\frac{C_{G,k,n}}{H_k} - C_{L,k,n} \right) - k_L a (C_{L,k,n} - C_{W,k,n}) + \frac{Q_L(t)}{V_L} (C_{L,k,\text{in}} - C_{L,k,n}), \quad (26)$$

and even $C_{L,k,\text{in}} = C_{L,k,1}$ if the liquid receptacle at the bottom is assumed as nonreactive. The other parameter involved is $k_L a$, the liquid mass transfer coefficient.

2.4 Biofilm model

In both moist and wet biofilms is where hydrogenotrophy reaction takes place, given by combined Monod kinetics:

$$\rho_{i,j}(t) = \rho_{\text{max}} \cdot \frac{C_{\text{H}_2,i,j}(t)}{K_{\text{H}_2} + C_{\text{H}_2,i,j}(t)} \cdot \frac{C_{\text{CO}_2,i,j}(t)}{K_{\text{CO}_2} + C_{\text{CO}_2,i,j}(t)}. \quad (27)$$

Therefore, differential equations for $j = 2, \dots, (p-1)$, presented here for the moist biofilm, are

$$\dot{C}_{k,i,j}(t) = \frac{D_k}{\theta^2} (C_{k,i,j-1}(t) - 2C_{k,i,j}(t) + C_{k,i,j+1}(t)) + r_k \rho_{i,j}(t), \quad (28)$$

where r_k is the stoichiometric coefficient for the k -th gas with $r_{\text{H}_2} < 0$, $r_{\text{CO}_2} < 0$ and $r_{\text{CH}_4} = 1$. For the innermost layer in contact with the inert support, i.e. for $j = p$, the differential equations change:

$$\dot{C}_{k,i,p}(t) = \frac{D_k}{\theta^2} (C_{k,i,p-1}(t) - C_{k,i,p}(t)) + r_k \rho_{i,p}(t). \quad (29)$$

For the wet biofilm, the equations are the same, but $j = p+3, \dots, 2p+1$ and the innermost layer is at $j = 2p+2$.

3. SIMULATION FITTING AND RESULTS

Experimental results to be fitted by the model, carried out by Muñoz-Páez et al. (2025), extended for a period of 69 days divided in 3 experimental phases, in all of which the liquid recirculation rate was kept at 160 ml/min in a cylindrical TFB. Phases 1, 2, and 3 used an empty bed residence time (EBRT) of 12, 6, and 3 hours respectively. Tables 2 and 3 list the physicochemical and biofilm parameters retrieved from (Dupnock and Deshusses, 2021), and those used for the model simulation³.

³ Symbol \star indicates measured parameters in Muñoz-Páez et al. (2025); and symbol \dagger denotes parameters adjusted to fit simulation results to experimental results therein.

Table 2. Physicochemical parameters

Symbol	Parameter	Value
T	Temperature	37.0 °C
P	Pressure	1.013 bar
*h	Reactor height	13.9 cm
*r	Reactor radius	4.0 cm
$^*V_{reactor}$	Total volume reactor	700 ml
$^*V_{Gtot}$	Total gaseous-space volume	$0.22 \cdot V_{reactor}$
$^*V_{Ltot}$	Total liquid volume	$0.08 \cdot V_{reactor}$
D_{ax}	Axial dispersion coefficient	1000 cm ² /h
$^{\dagger}k_{GA}$	Gas-liquid mass transfer coefficient	300 h ⁻¹
k_{La}	Liquid-biofilm mass transfer coefficient	4.3 h ⁻¹

3.1 Coarse tuning

Simulation was set assuming $n = 5$ levels for TFB, $p = 2$ biofilm layers, and 3 gases, which originated a system of $n \times (2p + 2) \times 3 = 90$ algebraic-differential equations to be solved using MATLAB[®]'s ode23s solver. Therefore, the total volume of the reactor was divided into $n = 5$ levels of volume $V_{G,i} = 140$ ml. with level height $\delta = 2.78$ cm. Proportions of gaseous space and liquid volumes for a level were assumed always constant and selected according to the best ratios addressed by Dupnock and Deshusses (2021). A simple method to establish the number of cylindrical levels considered to build the model, is to measure the difference of CH₄ volumetric proportions between levels $i = n$ and $i = n - 1$ after performing a simulation: if such difference was less than 1%, then n levels were suitable to construct the model. With the parameters considered, $n=3$ levels were deemed as adequate.

As per the biofilm thickness, many simulations revealed that the addition of multiple layers p has a negligible effect in the variability of concentrations on the biofilm layer in direct contact with both liquid and gaseous media; thus, keeping a low p avoids constructing a potentially large-size model that would require more computational effort.

Table 3. Biofilm parameters

Symbol	Parameter	Value
θ	Biofilm thickness	20 μ m
$^{\dagger}\rho_{max}$	Maximum reaction rate for H ₂	220 mg CH ₄ /(L·h)
K_{CO_2}	Michaelis-Menten constant for CO ₂	0.02 mg CO ₂ /L
K_{H_2}	Michaelis-Menten constant for H ₂	0.02 mg H ₂ /L
H_{H_2}	Henry's constant for H ₂ (37°C)	51
D_{H_2}	Diffusion coefficient for H ₂	0.16 cm ² /h
H_{CO_2}	Henry's constant for CO ₂ (37°C)	1.84
D_{CO_2}	Diffusion coefficient for CO ₂	0.069 cm ² /h
H_{CH_4}	Henry's constant for CH ₄ (37°C)	35
D_{CH_4}	Diffusion coefficient for CH ₄	0.015 cm ² /h

The time domain for simulation is spaced every hour, with 24 data points per day and simulation was set up to 72 simulation time days, since data from each experiment was obtained at day-end. Several resolutions of the differential equations took almost less than 3 seconds per time domain of 24 hours, which resulted in a maximum computing time of $72 \times 3s = 216s = 3.6$ min. executed in MATLAB 2022a on a 13rd. gen. Intel Core I5-1335U (12-CPU) 64bits processor with 16GB RAM. If influent proportions were constant, execution times were even 6 times shorter. Simulations considered small random changes from the

nominal composition of the influent gas to emulate the expected variations that occur naturally.

3.2 Fine tuning

Figure 3 presents as solid colored lines volumetric proportions in all levels for the three gases involved. For comparison with experimental data, measured volumetric proportions of each gas are depicted with red dots. As expected, the progressively upper location of the i -th level causes the amount of both H₂ and CO₂ to diminish as hydrogenotrophic methanization takes place and accumulates CH₄ along the predominant path of the gas flow (upwards), improving the purity of the resulting biomethane. In lower levels, concentrations of H₂ and CO₂ are greater as the raw biogas source is closer.

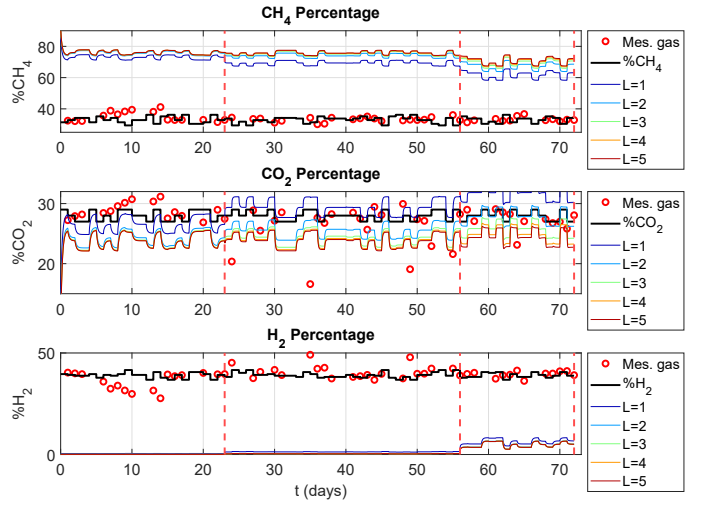


Fig. 3. Gaseous proportions in influent and TFB levels.

Drawn as solid black lines in Figure 3, gaseous influent volumetric proportions are depicted and they varied according to Figure 4 showing the H₂:CO₂ and CH₄:CO₂ gaseous influent volumetric ratios. Although it is deemed advisable to keep the influent proportions close to the theoretical stoichiometric ratio of H₂:CO₂=4, practical results suggest using volumetric ratios of $1.1 \leq H_2:CO_2 \leq 2$ to favour productivity of CH₄ by trading off some purity of the biomethane effluent (Muñoz-Páez et al., 2025).

The upper portion of Figure 5 depicts simulation results for effluent volumetric proportions plotted for all gases, and the volumetric proportions measured during the experiments plotted with point markers; the lower portion of Figure 5 presents simulation results of productivity for all gases expressed in L/(L_{reactor}/day), where measured methane in the effluent is signalled with point markers.

If the operational objective is to enhance the purity methane in the effluent, the volumetric influent ratios are sensitive parameters with a clear effect on the gaseous outflow. Although in practice they are not expected to vary abruptly, it is crucial to find a safe practical operating interval: in many run simulations, it was notorious that a volumetric ratio of almost the ideal stoichiometric ratio H₂:CO₂= 4:1 was detrimental for the proposed model, as CO₂ was depleted and an important amount of H₂ remained unconsumed in the gaseous effluent. This fact

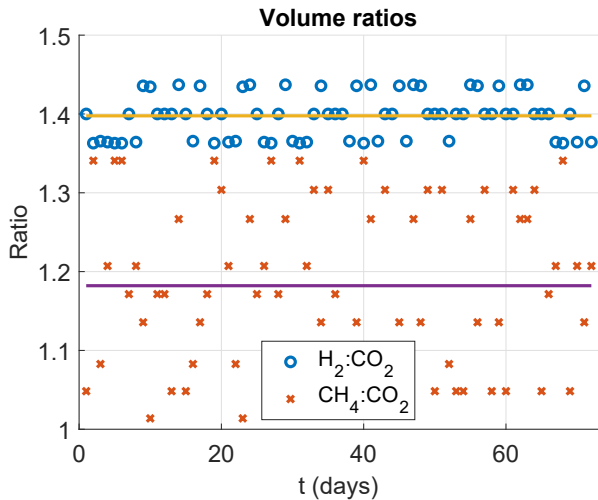


Fig. 4. Volumetric influent ratios.

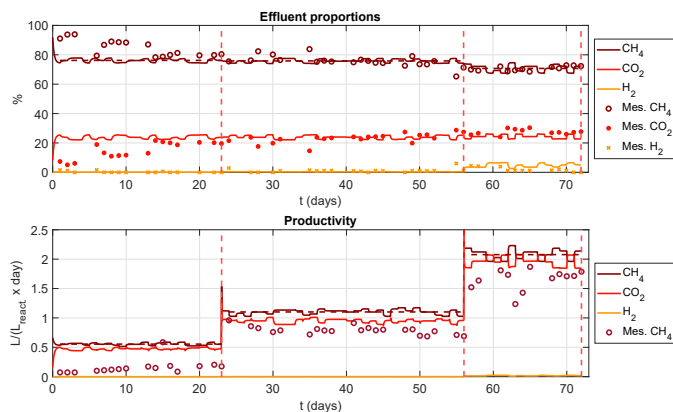


Fig. 5. Gaseous effluent proportions and CH_4 productivity.

was interesting to notice, since many works suggest the experimental use this ideal stoichiometric ratio.

Another key finding during the model refinement was: from (1), the stoichiometric coefficients should theoretically be $[r_{\text{CH}_4}, r_{\text{CO}_2}, r_{\text{H}_2}] = [1, -1, -4]$. However, the model required fitting these parameters for all three phases as $[r_{\text{CH}_4}, r_{\text{CO}_2}, r_{\text{H}_2}] = [1, -1.5, -4]$. A reason for this discrepancy may be that, in phases 1 and 2, activity of acetoclastic archaea was detected (Muñoz-Páez et al., 2025); thus, not only hydrogenotrophy is taking place and additional bioreactions could be added to the model, but they were disregarded to keep the model simple. It is more convenient to adjust the stoichiometric coefficients for each experimental phase.

4. CONCLUSIONS

A lumped-parameter model for a trickling filter bioreactor was proposed and simulated using MATLAB[®]. The execution time of the simulation resulted surprisingly faster than expected considering the potentially large-sized models originated using the presented approach. The simulation fitted remarkably well the experimental data originated from a 69 days experiment set up on the real trickling filter bioreactor, and model simulation condensed experimental time in an execution time of less than 3 minutes on average using a regular laptop. Hence, rapid execution times

allows to easily modify a parameter and to study, after a simulation, the response of the model to such parameter variation.

Simulation particularly fitted well the measured volumetric composition of gaseous effluent in the experiment. Productivity was not fitted as accurately as volumetric composition due to disregarding the influence of acetoclastic archaea in the model, which produce additional CO_2 , and due to also possible gaseous outflow proportions measurement errors; hence, simulation results for CH_4 productivity overestimated the measured productivity data of the experiment. In turn, qualitatively sensitive variables such as the volumetric influent $\text{H}_2:\text{CO}_2$ ratio; and parameters such as the kinetic reaction rate, and the stoichiometric coefficients were crucial for fitting the model. In contrast, considering multiple biofilm layers had almost no effect on productivity or composition of the gaseous effluent.

As suggested by experimental results in other works, several simulations evidenced that volumetric ratios for the gaseous influent near the stoichiometric ideal $\text{H}_2:\text{CO}_2 = 4:1$ for hydrogenotrophic methanation are detrimental for enhancing productivity and purity of biomethane. Diffusivity parameters defining Fickian diffusion were also relevant, but they are easily constrained due to physical limitations of influent flow, reactor volume, and liquid influent or mineral substrate liquid recirculation rate. Additional refinements of the model such as proposing other kinetic reaction functions, incorporation of variable liquid volume in the trickling filter levels, addition of gaseous outflow storage dynamics, or considering phenomena related to acetoclastic archaea could be further discussed.

REFERENCES

- Burkhardt, M. and Busch, G. (2013). Methanation of hydrogen and carbon dioxide. *Appl. En.*, 111, 74–79.
- Dupnock, T.L. and Deshusses, M.A. (2021). Development and validation of a comprehensive model for biotrickling filters upgrading biogas. *Chem. Eng. J.*, 407, 126614.
- Gujer, W. and Zehnder, A.J.B. (1983). Conversion processes in anaerobic digestion. *Water Sci. & Technol.*, 15, 127–167.
- Katariya, H.G. and Patolia, H.P. (2023). Advances in biogas cleaning, enrichment, and utilization technologies: a way forward. *Biomass Conversion & Biorefinery*, 13, 9565–9581.
- Markthaler, S., Plankenbühler, T., Weidlich, T., Neubert, M., and Karl, J. (2020). Numerical simulation of trickle bed reactors for biological methanation. *Chem. Eng. Sci.*, 226, 115847.
- Muñoz, R., Meier, L., Diaz, I., and Jeison, D. (2015). A review on the state-of-the-art of physical/chemical and biological technologies for biogas upgrading. *Reviews in Environmental Sci. and Bio/Technol.*, 14, 727–759.
- Muñoz-Páez, K.M., Ramos-Arechiga, K.Y., and Buitrón, G. (2025). Ex-situ biogas enrichment by hydrogenotrophic methanogens at low H_2/CO_2 ratios: Effect of empty bed residence time. *Fuel*, 381, 133330.
- Swinbourn, R., Li, C., and Wang, F. (2024). A comprehensive review on biomethane production from biogas separation and its techno-economic assessments. *Chemistry-Sustainability-Energy-Materials*, 17(19), e202400779.